Journal of Information Systems and Telecommunication
Vol.11, No.4, October-December 2023,294-306
http://jist.acecr.org
ISSN 2322-1437 / EISSN:2345-2773

A New Power Allocation Optimization for One Target Tracking in Widely Separated MIMO Radar

Mohammad Akhondi Darzikolaei[1*], Mohammad Reza Karami Mollaei[1] , Maryam Najimi[2]

[1] Department of Electrical and Computer Engineering, Babol Noshirvani University of Technology,Babol, Iran
[2].Department of Electrical and Computer Engineering, University of Science and Technology of Mazandaran,Behshahr, Iran

Received: 03 Oct 2022/ Revised: 04 Dec 2022/ Accepted: 18 Jan 2023

Abstract

In this paper, a new power allocation scheme for one target tracking in MIMO radar with widely dispersed antennas is designed. This kind of radar applies multiple antennas which are deployed widely dispersed from each other. Therefore, a target is observed simultaneously from different uncorrelated angles and it offers spatial diversity. In this radar, a target's radar cross section (RCS) is different in each transmit-receive path. So, a random complex Gaussian RCS is supposed for one target. Power allocation is used to allocate the optimum power to each transmit antenna and avoid illuminating the extra power in the environment and hiding it from interception. This manuscript aims to minimize the target tracking error with constraints on total transmit power and the power of each transmit antenna. For calculation of target tracking error, the joint Cramer Rao bound for a target velocity and position is computed and this is assumed as an objective function of the problem. It should be noted that a target RCS is also considered as unknown parameter and it is estimated along with target parameters. This makes a problem more similar to real conditions. After the investigation of the problem convexity, the problem is solved by particle swarm optimization (PSO) and sequential quadratic programming (SQP) algorithms. Then, various scenarios are simulated to evaluate the proposed scheme. The simulation results validate the accuracy and the effectiveness of the power allocation structure for target tracking in MIMO radar with widely separated antennas.

Keywords: unknown RCS; Target tracking; Power allocation; MIMO radar; Joint Cramer Rao bound; PSO; SQP

1- Introduction

Radar system applies eletromagnetic waves to assign target position, velocity, and other features [1-2]. In the last decades, MIMO radars become an important and attractive issue in radar research [3]. A MIMO radar uses multiple receiver and transmitter antennas to illuminate the specific waveform [4]. The superiority of MIMO radars over conventional radars has been recently proved in many aspects. These radars include of many transmitters and receivers located far from each other. In this scenario, the MIMO radar can observe the targets from different directions. One of the advantages of these radars is exploitation of Doppler frequencies from different transmitter-target-receiver paths. The extracted Doppler frequencies can be used for estimation of target parameters so that, the radar can track the targets with reasonable accuracy[5]. Collocated and widely separated antennas are the common types of MIMO radar. In the collocated type, the antennas are deployed so near, similar to Phased Array. In the widely separated MIMO radar, all antennas are deployed in a great geographical environment and target is observed from various uncorrelated aspect angles.

Power consumption is an essential challenge in wireless networks in UAV communications [6], underwater communications, cooperative cognitive radio netwrok [7], and radar systems. Power allocation is usually applied to allocate the optimum power value between the transmit antennas. to minimize the tracking error with power constraints in transmitter or its converse is a common strategy for power allocation scheme in MIMO radar system [8]. Power allocation is also essential to hiding the radar from other LPI radars [9]. Power allocation technique in MIMO radar systems is investigated in recent research. Using power allocation technique in MIMO radar with widely separated antennas is investigated in [10]. In target tracking cycle just target range is

✉ **Mohammad Reza karami Mollaei**
mkarami@nit.ac.ir

considered. The problem is constructed by aiming to maximize B-FIM1. it is derived and then the problem is formed as one cooperative game. Then, the problem is solved to distribute the total power between transmitting antennas. the selection of antennas and power allocation technique for localization in distributed type of MIMO radar are proposed in [11]. A constrained problem by aiming to minimize the estimation error of target position is solved. The transmit antenna number and power budget were the constraints of this problem. [12] Introduces a joint method in antenna selection for target tracking problem in distributed MIMO radar. Resource restrictions in radars make it essential to choose radars at per time cycle and maintain the performance in the high condition. Therefore, the PCRLB 2 is applied as an optimization criterion for this problem. [13] Proposes a new resource allocation technique for the multi-target tracking in widely separated MIMO radar and it considers just a velocity as an unknown parameter. The authors selected one key target. They applied the MSE of that target velocity estimation as an optimization problem criterion. The choosing of receive and transmit antennas and assigning of transmit power and signal time are the parameters that are obtained in this problem. [14] Considers a netted Collocated MIMO radar and suggests joint beam and power schemes for multi-target tracking. a distributed fusion is also used to reduce the communication requirements while keeping the system robustness. The distributed fusion schemes use covariance intersection fusion. [15] Designs a joint antenna placement and power allocation technique in MIMO radar with widely separated antennas to increase target detection performance. First, a problem for the Neyman-Pearson detector by using the Lagrange power allocation scheme and the antenna deployment optimization is considered. Then with the iterative method, the problem is solved. The power allocation scheme based on PSO for one target tracking strategy is introduced in [16]. The problem is formed for MIMO radar with widely dispersed antennas. The power allocation technique with aiming to minimize the tracking error with constraints on the total power and each transmit antenna power is constructed. Then with the PSO algorithm, that problem is solved. In this reference, the joint target position and velocity are considered unknown parameters and then the CRB of estimation error is calculated and it is used as an objective function. In [17], a solution for joint beam and power scheduling in the netted Collocated MIMO radar systems for distributed multi-target tracking is suggested. This solution contains a distributed fusion architecture that decreases the communication requirements while maintaining the overall robustness of the system. The distributed fusion architecture employs the covariance intersection fusion to address the unknown information correlations among radar nodes. An adaptive sensor scheduling integrated with power and bandwidth allocation is presented for centralized multiple target tracking in the netted collocated MIMO radar in [18].

By reviewing the above research, in this paper, we slove some challenges including using joint target velocity and position in the calculation of target tracking error, and considering random complex Gaussian target RCS. Besides considering these two challenges, we consider random complex Gaussian RCS as an unknown parameter and it is estimated along with the target position and velocity parameter. This is similar to real conditions. Because in other research, they consider RCS known but is obvious that we usually do not have any information from the target RCS. Therefore, the estimation of RCS is a very essential issue that should be performed in the estimation cycle. To our knowledge, this is the first time performed for power allocation problem for target tracking in MIMO radar with widely separated antennas.

The scope of this manuscript are including:

1. First, The system model and the antenna deployment model for widely separated MIMO radar are determined. Then target motion model is chosen. random model with complex Gaussian distribution is selected for target RCS and it is used in the computation of Cramer Rao bound for target parameters estimation error. And also, besides the target parameters, the target RCS is considered an unknown parameter. (This is the first time considered for MIMO radar with widely separated antennas). It is the essential assumption because target RCS depends on many target factors and it cannot be known and should be achieved in the estimation process.
2. CRB for unknown target parameters and the variance of random RCS are computed and then Joint CRB for target velocity and position estimation is obtained. The joint CRB has used an objective function for the power allocation problem.
3. The power allocation scheme is designed. The minimizing one target tracking errors by considering the transmit power of each transmit antenna and total transmit power limitations is the power allocation problem of this

[1] Bayesian fisher information matrix
[2] Posterior Cramer Rao lower bound

manuscript. We aim to minimize the tracking errors with the above constraints.
4.The PSO and SQP algorithm are utilized to slove this problem. These algorithms are formed to assign optimal value to each transmit antenna and satisfy the constraints in the problem.
The remainder of the paper is structured as follows:
the system model is mentioned in section 2. In the next, target parameters error is calculated. Part 4 constructs a power allocation problem and applies two SQP and PSO algorithms for solving it. Section 5 presents the simulation results, the conclusion comments are mentioned in section 6, and in the final part, the appendices are presented.

2- System Model

In this model, nth receive antenna is located in (x_n, y_n), where $n = 1,2, \ldots\ldots, N$. The position of the target is in (x_q, y_q) and the target velocity equals $(\dot{x}_q, \dot{y}_q)$. A set of orthogonal signals,$s_m(t)$, is illuminated. ($\int_{T_m} |s_m(t)|^2 dt = 1$). period, effective bandwidth and transmit power of mth transmit waveform are shown as T_m,β_m, P_m. RCS of mnth path is expressed as a zero-mean complex Gaussian random variable $\xi_{mn} \sim \mathcal{CN}(0, \sigma_{mn}^2)$. Where σ_{mn}^2 is the mnth path variance and we conisder it unknown in this paper.
The assumptions of this paper are as follow:
1. w_{mn} (Noise of mnth transmit-receive path) and ξ_{mn} in mn th paths are mutually independent.
2. the transmit signals are orthogonal. This also true for time delays and Doppler shifts [19]:
3. we consider $\sigma_w^2 = 1$.
4. The antennas are adequately spaced far [20]. Therefore, the observation of the target in each path is independent and RCS, ξ_{mn}, is independent.
The time delay of (m, n)th transmit-receive path in kth time slot is:

$$\tau_{mn,k} = \frac{d_{m,k} + d_{n,k}}{c} \tag{1}$$

And,

$$d_{m,k} \triangleq \sqrt{\left(x_{q,k} - x_m\right)^2 + \left(y_{q,k} - y_m\right)^2}$$
$$d_{n,k} \triangleq \sqrt{\left(x_{q,k} - x_n\right)^2 + \left(y_{q,k} - y_n\right)^2} \tag{2}$$

Where, c is light velocity. $d_{m,k}$ and $d_{n,k}$show the distance from mth transmitter and nth receiver from the target.
The received signal from mth transmit antenna at nth receive antenna at time k is:

$$r_{mn,k}(t) = \sqrt{\alpha_{mn,k} P_m}\ \xi_{mn,k}\ s_m\left(t - \tau_{mn,k}\right) e^{j2\pi f_{mn,k} t} + w_{mn,k}(t) \tag{3}$$

where, $w_{mn,k} \sim \mathcal{CN}(0, \sigma_w^2)$. The loss of pass is illustrated as $\alpha_{mn,k} = \frac{1}{(4\pi)^3} \frac{1}{f_c^2} \frac{1}{d_{m,k}^2\, d_{n,k}^2}$. Where f_c is the carrier frequency.
Doppler frequency in mn path and time-slot k can be expressed as:

$$f_{mn,k} = \frac{\dot{x}_{q,k}\left(x_m - x_{q,k}\right) + \dot{y}_{q,k}\left(y_m - y_{q,k}\right)}{\lambda d_{m,k}} + \frac{\dot{x}_{q,k}\left(x_n - x_{q,k}\right) + \dot{y}_{q,k}\left(y_n - y_{q,k}\right)}{\lambda d_{n,k}} \tag{4}$$

λ shows the wavelength.

2-1- Motion Model

The constant velocity (CV) is considered for the target motion model of this paper. This model expressed as [10]:

$$\boldsymbol{\theta}_{k+1} = \boldsymbol{F}\boldsymbol{\theta}_k + \boldsymbol{w}'_k \tag{5}$$

$\boldsymbol{\theta}_k = \left[x_{q,k}, \dot{x}_{q,k}, y_{q,k}, \dot{y}_{q,k}\right]^T$ is unknown target position and velocity vector. That it will be estimated in tracking cycle. $\boldsymbol{w}'_k$ is a Gaussian vector and represent noise and it is modeled as $\mathcal{N}(0, \boldsymbol{\Sigma}_k)$. Where $\boldsymbol{\Sigma}$ illustrates the covariance matrix, and **F** shows the state transition matrix [20]:

$$\boldsymbol{F} = \begin{bmatrix} 1 & \mathrm{T} & 0 & 0 \\ 0 & 1 & 0 & 0 \\ 0 & 0 & 1 & \mathrm{T} \\ 0 & 0 & 0 & 1 \end{bmatrix} \tag{6}$$

$$\boldsymbol{\Sigma} = \begin{bmatrix} \frac{\mathrm{T}^2}{3} & \frac{\mathrm{T}^2}{2} & 0 & 0 \\ \frac{\mathrm{T}^2}{2} & \mathrm{T} & 0 & 0 \\ 0 & 0 & \frac{\mathrm{T}^2}{3} & \frac{\mathrm{T}^2}{2} \\ 0 & 0 & \frac{\mathrm{T}^2}{2} & \mathrm{T} \end{bmatrix} \mathrm{l} \tag{7}$$

sample intervals and the process noise density are shown in T and l.
In this paper, besides$\boldsymbol{\theta}_k$, the target RCS in each transmit-receive path, $\xi_{mn,k}$, is also supposed to be unknown. Therefore, the unknown parameter vector is changed as:

$$\boldsymbol{\theta'}_k = \left[x_{q,k}, \dot{x}_{q,k}, y_{q,k}, \dot{y}_{q,k}, \boldsymbol{\xi}_k^T\right]^T \tag{8}$$

Where, $\boldsymbol{\xi}_k = \left[\xi_{11,k}, \xi_{12,k}, \ldots\ldots, \xi_{NM,k}\right]^T$. In this case, the state transition matrix is changed as $'$:

$$\boldsymbol{F'} = \begin{bmatrix} \boldsymbol{F} & \mathbf{0}_{\mathrm{n}_\theta \times \mathrm{NM}} \\ \mathbf{0}_{\mathrm{NM} \times \mathrm{n}_\theta} & \boldsymbol{I}_{NM} \end{bmatrix} \tag{9}$$

It is noted that the RCS transition model is like first-order Markov process and it is obtained as [21]:

$$\boldsymbol{\xi}_k = \boldsymbol{\xi}_{k-1} + \boldsymbol{\mu}_{k-1} \tag{10}$$

Where $\boldsymbol{\mu}_{k-1}$ white Gaussian noise with $\boldsymbol{Q}_{\xi,k-1}$ covariance. Therefore, according to (9), the unknown parameter transition model is achieved as:

$$\boldsymbol{\theta'}_k = \boldsymbol{F'}\boldsymbol{\theta'}_{k-1} + \boldsymbol{\eta}_{k-1} \quad (11)$$

Where in above equations, n_θ shows the dimension of the unknown parameter vector and $\boldsymbol{\eta}_{k-1}$ is Gaussian noise with covariance equals to $\boldsymbol{Q}_{\boldsymbol{\theta'}} = blkdiag\{\boldsymbol{\Sigma}, \boldsymbol{Q}_{\xi,k}\}$.
Since $\xi_{mn,k}$ is random variable with zero mean and $\sigma^2_{mn,k}$ variance, therefore, the $\sigma^2_{mn,k}$ is used in unknown parameter vector instead of $\xi_{mn,k}$:

$$\boldsymbol{\theta'}_{\mathrm{k}} = \left[x_{q,k}, \dot{x}_{q,k}, y_{q,k}, \dot{y}_{q,k}, , \sigma^2_{11,k}, \sigma^2_{12,k}, \dots., \sigma^2_{NM,k}\right]^T \quad (12)$$

In the next part, the joint CRB for target tracking error is calculated.

3- Joint CRB for Target Tracking Error

Log-likelihood ratio of the unknown parameter ($\boldsymbol{\theta}_{\mathrm{k}}$) is obtained as [13]:

$$\mathrm{L}_{mn}\left(\boldsymbol{\theta}_k; r_{mn}(t)\right) = Ln\,\Lambda_{mn}\left(\boldsymbol{\theta}_k; r_{mn,k}(t)\right) = \frac{\sigma^2_{mn}P_m}{\sigma^2_{mn}P_m + 1}\left|\int_{-\infty}^{+\infty} r_{mn,k}(t)\, s^*_m\big(t - \tau_{mn,k}\big)e^{-j2\pi f_{mn,k}t}\, dt\right|^2 + C_{mn} \quad (13)$$

Where $C_{mn} = -\ln(\sigma^2_{mn}P_m + 1)$, and $r_{mn,k}(t)$ shows the observation signal in nth receiver from mth transmitter
According to our assumptions, RCS and noise are independent, the joint likelihood ratio term are achieved by [13]:

$$\Lambda_J\left(\boldsymbol{\theta}_k; \boldsymbol{r_k}(t)\right) = \prod_{m=1}^{M}\prod_{n=1}^{N}\Lambda_{mn}\left(\boldsymbol{\theta}_k; r_{mn,k}(t)\right) \quad (14)$$

Where $\boldsymbol{r_k}(t)$ is expressed as [16]:

$$\boldsymbol{r_k}(t) = [r_{11,k}(t), r_{12,k}(t), \dots, r_{NM,k}(t)] \quad (15)$$

According to [19], BIM for unknown parameter vector $\boldsymbol{\theta}_k$ is as:

$$\mathbf{J}_{\mathrm{B}}(\boldsymbol{\theta}_{\mathrm{k}}) = [\boldsymbol{\Sigma} + \mathbf{F}\,\mathbf{J}_{\mathrm{B}}^{-1}(\boldsymbol{\theta}_{\mathrm{k-1}})\,\mathbf{F}^{\mathrm{T}}]^{-1} + \mathbb{E}[\mathbf{J}_{\mathrm{D}}(\boldsymbol{\theta}_{\mathrm{k}})] \quad (16)$$

Where $\mathbf{J}_{\mathrm{D}}$ represents the Fisher Information Matrix (FIM). For the CRB calculation, first, FIM is calculated [23]:

$$\mathbf{J}_{\mathrm{D}}(\boldsymbol{\theta}_{\mathrm{k}}) = \mathbb{E}_{\boldsymbol{r_k}(t);\boldsymbol{\theta}_k}\{\nabla_{\boldsymbol{\theta}_k}\ln\Lambda_J(\boldsymbol{r_k}(t);\boldsymbol{\theta}_k)[\nabla_{\boldsymbol{\theta}_k}\ln\Lambda_J(\boldsymbol{r_k}(t);\boldsymbol{\theta}_k)]^T\} = -\mathbb{E}_{\boldsymbol{r_k}(t);\boldsymbol{\theta}_k}\{\nabla_{\boldsymbol{\theta}_k}[\nabla_{\boldsymbol{\theta}_k}\ln\Lambda_J(\mathbf{r_k}(t);\boldsymbol{\theta}_k)]^T\} \quad (17)$$

Since (13) is the function of $\tau_{mn,k}$ and $f_{mn,k}$, a new unknown parameter is defined as :

$$\boldsymbol{\vartheta'}_k = \left[\tau_{11,k}, \tau_{12,k}, \dots, \tau_{NM,k}, f_{11,k}, f_{12,k}, \dots, f_{NM,k}, \sigma^2_{11,k}, \sigma^2_{12,k}, \dots., \sigma^2_{NM,k}\right]^T \quad (18)$$

According to Chain rule, a new FIM is as:

$$\mathbf{J}_{\mathrm{D}}(\boldsymbol{\theta'}_{\mathrm{k}}) = \left(\nabla_{\boldsymbol{\theta'}_k}\boldsymbol{\vartheta'}_k{}^T\right)\mathbf{J}_{\mathrm{D}}(\boldsymbol{\vartheta'}_k)\left(\nabla_{\boldsymbol{\theta'}_{\mathrm{k}}}\boldsymbol{\vartheta'}_k{}^T\right)^T \quad (19)$$

$\nabla_{\boldsymbol{\theta'}_k}\boldsymbol{\vartheta'}_k{}^T$ Is calculated as (20).

$$\nabla_{\boldsymbol{\theta'}_k}\boldsymbol{\vartheta'}_k{}^T = \begin{bmatrix} \frac{\partial\tau_{11,k}}{\partial x_{q,k}} & \frac{\partial\tau_{12,k}}{\partial x_{q,k}} & \dots & \frac{\partial\tau_{NM,k}}{\partial x_{q,k}} & \frac{\partial f_{11,k}}{\partial x_{q,k}} & \frac{\partial f_{12,k}}{\partial x_{q,k}} & \dots & \frac{\partial f_{NM,k}}{\partial x_{q,k}} & 0 & \dots & 0 \\ \frac{\partial\tau_{11,k}}{\partial y_{q,k}} & \frac{\partial\tau_{12,k}}{\partial y_{q,k}} & \dots & \frac{\partial\tau_{NM,k}}{\partial y_{q,k}} & \frac{\partial f_{11,k}}{\partial y_{q,k}} & \frac{\partial f_{12,k}}{\partial y_{q,k}} & \dots & \frac{\partial f_{NM,k}}{\partial y_{q,k}} & 0 & \dots & 0 \\ 0 & 0 & \dots & 0 & \frac{\partial f_{11,k}}{\partial \dot{x}_{q,k}} & \frac{\partial f_{12,k}}{\partial \dot{x}_{q,k}} & \dots & \frac{\partial f_{NM,k}}{\partial \dot{x}_{q,k}} & 0 & \dots & 0 \\ 0 & 0 & \dots & 0 & \frac{\partial f_{11,k}}{\partial \dot{y}_{q,k}} & \frac{\partial f_{12,k}}{\partial \dot{y}_{q,k}} & \dots & \frac{\partial f_{NM,k}}{\partial \dot{y}_{q,k}} & 0 & \dots & 0 \\ 0 & 0 & \dots & 0 & 0 & 0 & \dots & 0 & 1 & \dots & 1 \end{bmatrix}_{5\times 3NM} \quad (20)$$

The number of 0 and 1 in the right side of above matrix is NM. The above matrix parameters are calculated in [16]. By defining $\mathbf{J}_{\mathrm{D}}(\boldsymbol{\vartheta'}_k)$ as:

$$\mathbf{J}_{\mathrm{D}}(\boldsymbol{\vartheta'}_k) = \begin{bmatrix} \boldsymbol{G}_{11} & \boldsymbol{G}_{12} & \boldsymbol{G}_{13} \\ \boldsymbol{G}_{21} & \boldsymbol{G}_{22} & \boldsymbol{G}_{23} \\ \boldsymbol{G}_{31} & \boldsymbol{G}_{32} & \boldsymbol{G}_{33} \end{bmatrix} \quad (21)$$

Where, $\boldsymbol{G}_{11}$ contains second-order derivatives with respect to $\tau_{mn,k}$, $\boldsymbol{G}_{12}, \boldsymbol{G}_{21}$ are second-order derivatives with respect to $\tau_{mn,k}$ and $f_{mn,k}$, $\boldsymbol{G}_{22}$ is second-order derivatives with respect to $f_{mn,k}$, $\boldsymbol{G}_{13}, \boldsymbol{G}_{31}$ are second-order derivatives with respect to $\tau_{mn,k}$ and $\sigma^2_{mn,k}$, $\boldsymbol{G}_{23}, \boldsymbol{G}_{32}$ includes second-order derivatives with respect to $f_{mn,k}$ and $\sigma^2_{mn,k}$, and $\boldsymbol{G}_{33}$ contains second-order derivatives with respect to $\sigma^2_{mn,k}$ for all m and n in time slot k.. Therefore, (we show the proof procedure in **Appendix I**):

$$\boldsymbol{G}_{11} = \boldsymbol{C}\odot(\boldsymbol{I}_N \otimes diag\,\{\epsilon_1, \epsilon_2, \dots, \epsilon_M\}) \quad (22)$$
$$\boldsymbol{G}_{12} = \boldsymbol{G}_{21} = \boldsymbol{C}\odot diag\left\{\gamma_{11,k}, \gamma_{12,k}, \dots, \gamma_{NM,k}\right\} \quad (23)$$
$$\boldsymbol{G}_{22} = \boldsymbol{C}\odot diag\left\{\eta_{11,k}, \eta_{12,k}, \dots, \eta_{NM,k}\right\} \quad (24)$$
$$\boldsymbol{G}_{13} = \boldsymbol{G}_{31} = \boldsymbol{C_1}\odot(\boldsymbol{I}_N \otimes diag\,\{\chi_1, \chi_2, \dots, \chi_m\}) \quad (25)$$
$$\boldsymbol{G}_{23} = \boldsymbol{G}_{32} = \boldsymbol{C_1}\odot diag\left\{\varpi_{11,k}, \varpi_{12,k}, \dots, \varpi_{NM,k}\right\} \quad (26)$$
$$\boldsymbol{G}_{33} = \boldsymbol{C_2} \quad (27)$$

Where,

$$\boldsymbol{C} = 8\pi^2\, diag\,\{\frac{\sigma^4_{11}P^2_1}{\sigma^2_{11}P_1 + 1}, \dots., \frac{\sigma^4_{MN}P^2_M}{\sigma^2_{MN}P_M + 1}\} \quad (28)$$

$$\boldsymbol{C_1} = 4\pi\, diag\,\{\frac{\sigma^2_{11}P^2_1}{\sigma^2_{11}P_1 + 1}, \dots., \frac{\sigma^2_{MN}P^2_M}{\sigma^2_{MN}P_M + 1}\} \quad (29)$$

$$\boldsymbol{C_2} = diag\{\frac{2P_1^2}{\sigma_{11}^2 P_1 + 1}, \ldots, \frac{2P_M^2}{\sigma_{MN}^2 P_M + 1}\} \quad (30)$$

And also:

$$\chi_{m,k} = -j(\int f|S_m(f)|^2 df) \quad (31)$$

$$\varpi_{mn,k} = j\left(\int_{-\infty}^{+\infty} t \mid s_m^*(t-\tau_{mn,k})\right|^2 dt\Big) \quad (32)$$

$$\epsilon_m = \int_{-\infty}^{+\infty} f^2 |S_m(f)|^2 \, df - \left|\int_{-\infty}^{+\infty} f |S_m(f)|^2 \, df\right|^2 \quad (33)$$

$$\gamma_{mn,k} = \frac{1}{2\pi} \Im\{ \int_{-\infty}^{+\infty} t \, s_m^*(t - \tau_{mn,k}) \frac{\partial s_m(t-\tau_{mn,k})}{\partial \tau_{mn,k}} dt \} - \int_{-\infty}^{+\infty} f |S_m(f)|^2 \, df \cdot \int_{-\infty}^{+\infty} t \left|s_m(t-\tau_{mn,k})\right|^2 dt \quad (34)$$

$$\eta_{mn,k} = \int_{-\infty}^{+\infty} t^2 \left|s_m(t-\tau_{mn,k})\right|^2 dt - \left|\int_{-\infty}^{+\infty} t \left|s_m(t-\tau_{mn,k})\right|^2 dt\right|^2$$

Where, $S_m(f)$ denotes a Fourier transform of $s_m(t)$.
If we divide the $\nabla_{\boldsymbol{\theta'}_k} \boldsymbol{\vartheta'}_k{}^T$ to matrix block as:

$$\nabla_{\boldsymbol{\theta'}_k} \boldsymbol{\vartheta'}_k{}^T = \begin{bmatrix} \boldsymbol{A} & \boldsymbol{B} & \boldsymbol{0} \\ \boldsymbol{0} & \boldsymbol{D} & \boldsymbol{0} \\ \boldsymbol{0_{NM}} & \boldsymbol{0_{NM}} & \boldsymbol{1_{NM}} \end{bmatrix} \quad (36)$$

Where, $\boldsymbol{A}, \boldsymbol{B}, \boldsymbol{D}, \boldsymbol{0}$ are the $2 \times NM$ matrices and $\boldsymbol{0_{NM}}$ and $\boldsymbol{1_{NM}}$ are zero and one vectors with $1 \times NM$ dimension.

Since $\mathbf{J}_{\mathrm{D}}(\boldsymbol{\vartheta'}_k) = \begin{bmatrix} \boldsymbol{G_{11}} & \boldsymbol{G_{12}} & \boldsymbol{G_{13}} \\ \boldsymbol{G_{21}} & \boldsymbol{G_{22}} & \boldsymbol{G_{23}} \\ \boldsymbol{G_{31}} & \boldsymbol{G_{32}} & \boldsymbol{G_{33}} \end{bmatrix}$, therefore:

$$\boldsymbol{J_D}(\boldsymbol{\theta'}_k) = \begin{bmatrix} \mathbf{A} & \mathbf{B} & \mathbf{0} \\ \mathbf{0} & \mathbf{D} & \mathbf{0} \\ \mathbf{0_{NM}} & \mathbf{0_{NM}} & \mathbf{1_{NM}} \end{bmatrix} \begin{bmatrix} \mathbf{G_{11}} & \mathbf{G_{12}} & \mathbf{G_{13}} \\ \mathbf{G_{21}} & \mathbf{G_{22}} & \mathbf{G_{23}} \\ \mathbf{G_{31}} & \mathbf{G_{32}} & \mathbf{G_{33}} \end{bmatrix} \begin{bmatrix} \mathbf{A} & \mathbf{B} & \mathbf{0} \\ \mathbf{0} & \mathbf{D} & \mathbf{0} \\ \mathbf{0_{NM}} & \mathbf{0_{NM}} & \mathbf{1_{NM}} \end{bmatrix}^{\mathrm{T}} \quad (37)$$

And

$$\boldsymbol{J_D}(\boldsymbol{\theta'}_k) = \quad (38)$$

$$\begin{bmatrix} \mathbf{AG_{11}A^T + BG_{21}A^T + AG_{12}B^T + BG_{22}B^T} & \mathbf{AG_{12}D^T + BG_{22}D^T} & \mathbf{AG_{13}1_{NM}^T + BG_{23}1_{NM}^T} \\ \mathbf{DG_{21}A^T + DG_{22}B^T} & \mathbf{DG_{22}D^T} & \mathbf{DG_{23}1_{NM}^T} \\ \mathbf{1_{NM}G_{31}A^T + 1_{NM}^T G_{32}B^T} & \mathbf{1_{NM}G_{32}D^T} & \mathbf{1_{NM}G_{33}1_{NM}^T} \end{bmatrix}$$

After making block matrix:

$$\boldsymbol{J_D}(\boldsymbol{\theta'}_k) = 8\pi^2 \sum_{\boldsymbol{m=1}}^{\boldsymbol{M}} \sum_{\boldsymbol{n=1}}^{\boldsymbol{N}} \frac{\sigma_{mn}^4 P_m^2}{\sigma_{mn}^2 P_m + 1} \begin{bmatrix} \boldsymbol{J}_{Dnew}^{\boldsymbol{UL}} & \boldsymbol{J}_{Dnew}^{\boldsymbol{UR}} \\ \boldsymbol{J}_{Dnew}^{\boldsymbol{LL}} & \boldsymbol{J}_{Dnew}^{\boldsymbol{LR}} \end{bmatrix} \quad (39)$$

Therefore, $\mathbf{J}_{\mathrm{Dnew}}^{\boldsymbol{UL}}$, $\mathbf{J}_{\mathrm{Dnew}}^{\boldsymbol{UR}}$, $\mathbf{J}_{\mathrm{Dnew}}^{\boldsymbol{LL}}$, and $\mathbf{J}_{\mathrm{Dnew}}^{\boldsymbol{LR}}$ are obtained in (40), (41), (42), and (43).

$$\mathbf{J}_{\mathrm{Dnew}}^{\boldsymbol{UR}} = (\frac{1}{2\pi\sigma_{mn}^2}) \begin{bmatrix} \sum_{\boldsymbol{m=1}}^{\boldsymbol{M}} \sum_{\boldsymbol{n=1}}^{\boldsymbol{N}} (a_{mn,k}\chi_{m,k} - e_{mn,k}\varpi_{mn,k}) \\ \sum_{\boldsymbol{m=1}}^{\boldsymbol{M}} \sum_{\boldsymbol{n=1}}^{\boldsymbol{N}} (b_{mn,k}\chi_{m,k} - g_{mn,k}\varpi_{mn,k}) \\ -V_{mn,k}\varpi_{mn,k} \\ -q_{mn,k}\varpi_{mn,k} \end{bmatrix} \quad (41)$$

$$\boldsymbol{J}_{Dnew}^{\boldsymbol{LL}} = \left(\frac{1}{2\pi\sigma_{mn}^2}\right) \times \quad (42)$$

$$\left[\sum_{\boldsymbol{m=1}}^{\boldsymbol{M}} \sum_{\boldsymbol{n=1}}^{\boldsymbol{N}} (a_{mn,k}\chi_{m,k} - e_{mn,k}\varpi_{mn,k}) \quad \sum_{\boldsymbol{m=1}}^{\boldsymbol{M}} \sum_{\boldsymbol{n=1}}^{\boldsymbol{N}} (b_{mn,k}\chi_{m,k} - g_{mn,k}\varpi_{mn,k}) \quad -V_{mn,k}\varpi_{mn,k} \quad -q_{mn,k}\varpi_{mn,k}\right] \quad (35)$$

$$\mathbf{J}_{\mathrm{Dnew}}^{\boldsymbol{LR}} = \left(\frac{MN}{4\pi^2\sigma_{mn}^4}\right) \quad (43)$$

We can reform the (39) as :

$$\mathbf{J}_{\mathrm{D}}(\boldsymbol{\theta'}_{\mathrm{k}}) = \sum_{m=1}^{M} \sum_{n=1}^{N} 8\pi^2 \frac{\sigma_{mn}^4 P_m^2}{\sigma_{mn}^2 P_m + 1} \cdot (\mathrm{G_{mn}})_{5\times 5} \quad (44)$$

Where $\mathrm{G_{mn}}$ is function of target velocity and position and target RCS. $\mathbf{J}_{\mathrm{D}}(\boldsymbol{\theta'}_{\mathrm{k}})$ is 5×5 block matrix which is function transmit power of transmit antenna.
In the next part, the power allocation problem is constructed.

4- Power Allocation

In the construction of the power allocation problem, trace of Cramer Rao Bound matrix is considered as tracking error and it is obtained as:

$$\mathbb{F}_{\mathrm{B}}(\boldsymbol{\theta'}_k, \boldsymbol{P}) = \quad (45)$$
$$\mathrm{trace}(\boldsymbol{\Upsilon}_{\mathrm{k}}([\boldsymbol{J}_D^{-1}(\boldsymbol{\theta'}_k)]_{1,1} + [\boldsymbol{J}_D^{-1}(\boldsymbol{\theta'}_k)]_{2,2} + [\boldsymbol{J}_D^{-1}(\boldsymbol{\theta'}_k)]_{3,3} + [\boldsymbol{J}_D^{-1}(\boldsymbol{\theta'}_k)]_{4,4}\boldsymbol{\Upsilon}_{\mathrm{k}}^{\mathrm{T}})$$

Where, $[\boldsymbol{J}_D^{-1}(\boldsymbol{\theta'}_k)]_{1,1}$, $[\boldsymbol{J}_D^{-1}(\boldsymbol{\theta'}_k)]_{2,2}$, $[\boldsymbol{J}_D^{-1}(\boldsymbol{\theta'}_k)]_{3,3}$, and $[\boldsymbol{J}_D^{-1}(\boldsymbol{\theta'}_k)]_{4,4}$ are the CRB (lower bound) of the variance

$$\mathbf{J}_{\mathrm{Dnew}}^{\boldsymbol{UL}} = \quad (40)$$
$$\begin{bmatrix} \epsilon_m a_{mn,k}^2 + 2\gamma_{mn,k} a_{mn,k} e_{mn,k} + \eta_{mn,k} e_{mn,k}^2 & (\epsilon_m a_{mn,k} + \gamma_{mn,k} e_{mn,k}) b_{mn,k} + (\gamma_{mn,k} a_{mn,k} + \eta_{mn,k} e_{mn,k}) g_{mn,k} & (\gamma_{mn,k} a_{mn,k} + \eta_{mn,k} e_{mn,k}) V_{mn,k} & (\gamma_{mn,k} a_{mn,k} + \eta_{mn,k} e_{mn,k}) q_{mn,k} \\ (\epsilon_m a_{mn,k} + \gamma_{mn,k} e_{mn,k}) b_{mn,k} + (\gamma_{mn,k} a_{mn,k} + \eta_{mn,k} e_{mn,k}) g_{mn,k} & \epsilon_m b_{mn,k}^2 + 2\gamma_{mn,k} b_{mn,k} g_{mn,k} + \eta_{mn,k} g_{mn,k}^2 & (\gamma_{mn,k} b_{mn,k} + \eta_{mn,k} g_{mn,k}) V_{mn,k} & (\gamma_{mn,k} b_{mn,k} + \eta_{mn,k} g_{mn,k}) q_{mn,k} \\ (\gamma_{mn,k} a_{mn,k} + \eta_{mn,k} e_{mn,k}) V_{mn,k} & (\gamma_{mn,k} b_{mn,k} + \eta_{mn,k} g_{mn,k}) V_{mn,k} & \eta_{mn,k} V_{mn,k}^2 & \eta_{mn,k} V_{mn,k} q_{mn,k} \\ (\gamma_{mn,k} a_{mn,k} + \eta_{mn,k} e_{mn,k}) q_{mn,k} & (\gamma_{mn,k} b_{mn,k} + \eta_{mn,k} g_{mn,k}) q_{mn,k} & \eta_{mn,k} V_{mn,k} q_{mn,k} & \eta_{mn,k} q_{mn,k}^2 \end{bmatrix}$$

of target position and also target velocity in axis of x and y in kth frame. and $\mathbf{P} = [P_1, \dots, P_M]$ is a transmit antenna power vector, $\boldsymbol{\Upsilon}_k$ shows the normalization matrix and the target tracking error is illustrated in $\mathbb{F}_B$. $\boldsymbol{\Upsilon}_k$ is introduced as $\boldsymbol{\Upsilon}_k = I_2 \otimes \begin{bmatrix} 1 & 0 \\ 0 & T \end{bmatrix}$, Where I_2 is 2×2 identity matrix and $\otimes$ denotes the Kronecker product operator.

Our power allocation problem for target tracking in widely separated MIMO Radar by applying random Gaussian RCS and also considering target RCS as unknown parameter is expressed as:

$$\min_{P_m} \mathbb{F}_B(\boldsymbol{\theta'}_k, \boldsymbol{P}) \quad (46)$$

$$s.t. \sum_{m=1}^{M} P_m \le P_T \quad (47)$$

$$P_{min} \le P_m \le P_{max} \quad , m = 1,2, \dots, M \quad (48)$$

the first constraint of this problem shows that the sum of transmit powers is lower than a predetermined value, P_T. since MIMO radar wants to utilize the least power for one target tracking and it avoids to being intercepted. another constraint illustrates that each transmit antenna also has power limitation. To solve the (46) subject to (47) and (48), we use PSO and SQP algorithms. In **appendix III**, we prove that the problem is convex. The overall structure of solving the power allocation problem of this paper is illustrated in Fig.1.

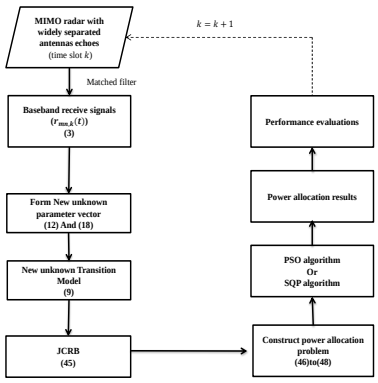

Fig.1. The Overall Structure of Solving the Power Allocation Problem of This Paper

4-1- The Problem Solution Based on PSO

The PSO algorithm [25] is based on animal's social behavior. The swarms construct a cooperative approach to find food and each member keeps varying the search pattern based on the learning experiences of its own and others. The pseudo code of algorithm to solve the problem of this paper is described in Algorithm1.

Algorithm1 The pseudo-code of PSO algorithm for this problem solution

1.Initialize parameters $(M, N, K, dimension(nvar), popsize, Maxiter, \omega, c_1, c_2, \omega_{damp}, P_{min}, P_{max})$

2. Uniformly randomly initialize each P_m in the population

$$par.var = P_{min} + (P_{max} - P_{min}). * rand(1, nvar) \quad (49)$$

3. define initial velocities randomly for each particle

$$par.vel = 0 \quad (50)$$

4. the fitness evaluation of each particle with the Cost function (51)

$$Cost(P_m) = \mathbb{F}_B(\boldsymbol{\theta'}_k, \mathbf{P}) + \gamma * (\sum_{m=1}^{M} P_m - P_T) \quad (51)$$

(Note that γ is a great value coefficient, to illustrate better constraint (47) in (46)).

$$par.cost = Cost(par.var) \quad (52)$$

5. define p_{best} and g_{best} in population and time slot (k) (in this paper is the minimum case)

6. while $iter < Maxiter$ do

7. for $k = 1{:}K$

8. for $i = 1{:}popsize$

9. Update velocity

$$par(i).vel = w * par(i).vel + \dots c1 * rand * (bpar(i).var - par(i).var) + \dots c2 * rand * (gpar(k).var - par(i).var); \quad (53)$$

10. Update variable

$$par(i).var = par(i).var + par(i).vel; \quad (54)$$

11. over merge checking

$$par(i).var = min(par(i).var, P_{max}) \quad (55)$$

$$par(i).var = max(par(i).var, P_{min}) \quad (56)$$

12. Compute the fitness values of new particle P_m with the Cost function (51)

$$par(i).cost = Cost(par(i).var) \quad (57)$$

13. If new particle value from (57) is better than p_{best} and p_{best} is better than g_{best} ,

Define new P_m as an optimal variable.

```
if par(i).cost < bpar(i).cost
    bpar(i) = par(i)
    if bpar(i).cost < gpar(k).cost
        gpar(k) = bpar(i);
    End if
End if
```
(58)

14. update decreasing coefficient ω

$$\omega = \omega * \omega_{damp} \quad (59)$$

15. End (for k)

16. End (for i)

17. $iter = iter + 1$;

18. End (while)

4-2- The Problem Solution Based on SQP

To prove the performance of first algorithm, and also because the problem is convex, we use another algorithm named SQP. In addition, the time complexity of PSO is

usually high and the SQP has less time consumption, we prefer to utilize SQP and compare these two algorithm results for our power allocation problem.

The structure of SQP algorithm for nonlinear problem is described as [24]:

$$\text{Min: } f(\mathbf{x}) \quad (60)$$

$$\text{s.t: } g_i(\mathbf{x}) \le 0, \quad i = 1, \dots, n_g \quad (61)$$

$$h_i(\mathbf{x})=0, \quad i = 1, \dots, n_h \quad (62)$$

$$x^l < \mathbf{x} < x^u \quad (63)$$

Where, f denotes an objective function, g and h show the inequality and equality function and $f, g,$ and h are twice continuously differentiable. $\boldsymbol{x}$ is the favorable variable matrix and it is limited by upper and lower bound x^u and x^l.

$\boldsymbol{\lambda}^k$ and $\boldsymbol{\nu}^k \ge 0$ are the Lagrange coefficients. Consider the below QP sub-problem as a direct extension of QP($\boldsymbol{x}^k, \boldsymbol{\lambda}^k$):

$$min_{\mathbf{d}^k} f(\mathbf{x}^k) + \nabla f(\mathbf{x}^k)^T \mathbf{d}^k + \frac{1}{2}\mathbf{d}^{kT}\nabla^2_{xx}\mathcal{L}(\mathbf{x}^k, \boldsymbol{\lambda}^k, \boldsymbol{\nu}^k) \quad (64)$$

$$\mathbf{d}^k$$

$$s.t.\ g_i(\mathbf{x}) + \nabla g_i(\mathbf{x}^k)^T \mathbf{d}^k = 0, \quad i = 1, \dots, n_g \quad (65)$$

$$h_i(\mathbf{x}) + \nabla h_i(\mathbf{x}^k)^T \mathbf{d}^k = 0, \quad i = 1, \dots, n_h \quad (66)$$

(53) is named as QP($\boldsymbol{x}^k, \boldsymbol{\lambda}^k, \boldsymbol{\nu}^k$) and $\mathcal{L}(\boldsymbol{x}^k, \boldsymbol{\lambda}^k, \boldsymbol{\nu}^k) = f(\boldsymbol{x}) + \boldsymbol{\nu}^T \boldsymbol{g}(\boldsymbol{x}) + \boldsymbol{\lambda}^T \boldsymbol{h}(\boldsymbol{x})$.

In this paper, problem (46) is the objective function and P_m is our favorable variable. (46) is f in (60) and $\mathbf{P}$ in (46) is $\boldsymbol{x}$ in (60). By supposing $\sum_{m=1}^{M} P_m - P_T \le 0$, we can say that $\boldsymbol{g}(\boldsymbol{x})$ in (61) is equal to $\sum_{m=1}^{M} P_m - P_T$ in our problem. Fig.2 shows the flowchart of SQP algorithm which is used in this paper.

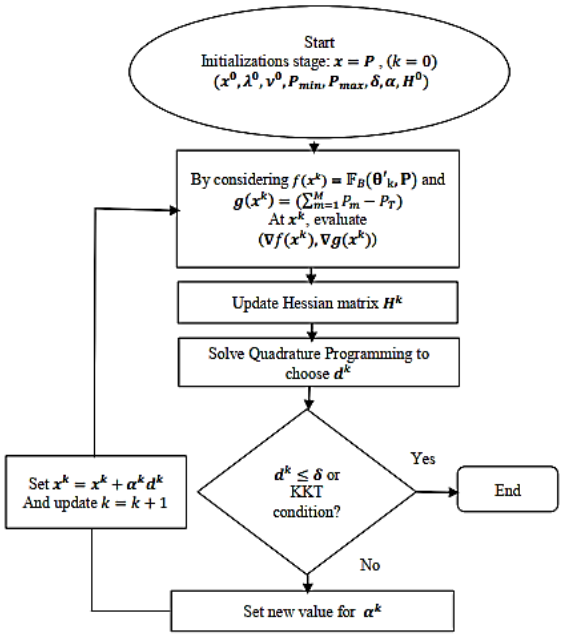

Fig.2. The Flowchart of SQP Algorithm for Solving the Problem of this Paper

5- Simulations

We perform some experiments to evaluate the proposed power allocation scheme. All the simulations are performed by Matlab software. In this paper, two symmetric and one asymmetric geometrical antenna placement scenarios are considered to illustrate the effect of antenna placement on tracking performance. Fig. 3 shows these two symmetric schemes for a MIMO radar with $M = 4$ and $N = 4$. To analyze the effect of the number of antennas on target tracking performance, it is considered another symmetric scenario with $M = 6$ and $N = 6$. Fig.4 shows this antenna placement geometry.

In symmetric cases, all antennas have ten kilometers distance from the origin. P_T equals 10 $Kwatt$. The carrier frequency is considered $9GHz$. σ^2_{mn} is supposed random and unknown parameter and in each transmit-receive path, it is different (in other research, for simplicity, it is usually considered one and known). $l = 0.1$ and $T = 0.2s$. The initial value for target location and velocity in x and y axis is $[500m\ 1000m\ 50\frac{m}{s}\ \ 30\frac{m}{s}]$. $P_{min} = 0.02P_T$ and $P_{max} = 0.8P_T$(watt).

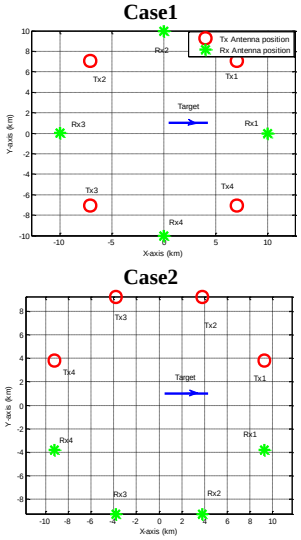

Fig.3 Symmetric Antenna Geometry Placement (M = 4, N = 4)

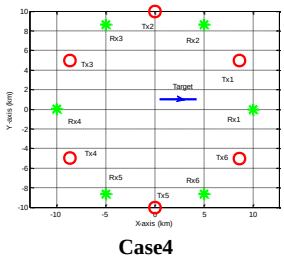

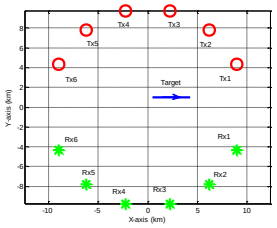

Fig.4 Symmetric Antenna Geometry Placement (M = 6, N = 6)

In Fig.5. We consider asymmetric antenna placement for a MIMO radar with $(M = 6, N = 6)$.

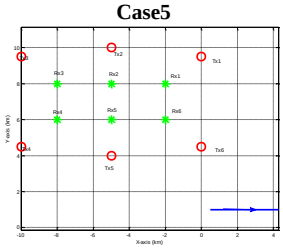

Fig.5 Asymmetric Antenna Geometry Placement (M = 6, N = 6)

To evaluate the proposed power allocation scheme for target tracking in widely separated MIMO radar, first, we apply PSO algorithm and extract the results. In Fig.6, the transmit power percentage of each transmit antenna in five considered cases (1 to 5) is shown. We can realize from Fig.6 that by moving the target toward the transmit antenna, the more power is allocated to that antenna. Therefore, in Case1, the transmit antenna 1and 4, in Case2, the transmit antenna 1and 2, in Case3, the transmit antenna 1and 6, in Case4, the transmit antenna 1and 2, and in Case5, the transmit antenna 1 and 6, take more power to have a better target tracking performance. In symmetric Cases (1 to 4), if the target is placed in (0,0), the power is equally distributed among transmit antennas.

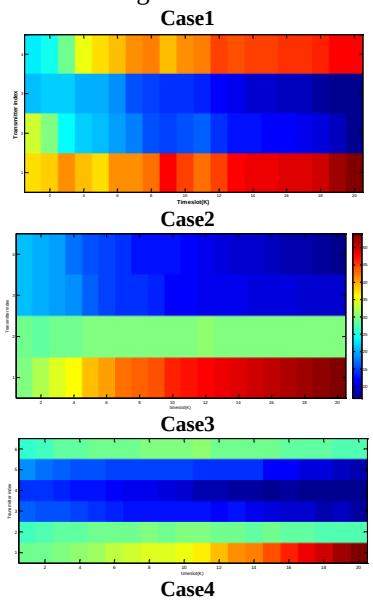

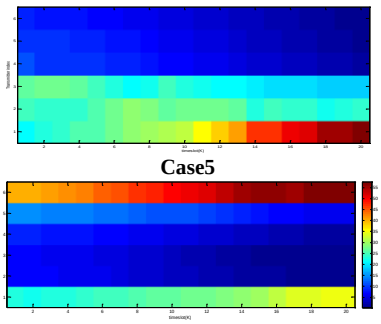

Fig.6. Each Transmit Antenna Power Percentage in Five Cases in Different Timeslots (based on PSO-based PP strategy)

Fig.7 illustrates that the proposed power allocation strategy (based on the PSO algorithm) has better performance and the less CRB of target tracking error than other schemes such as uniform and random power allocation. We can see this priority in all cases (Case1 (a), Case2 (b), Case3 (c), Case4 (d), and Case5 (e) in Fig.7). By attention to this figure, we can realize that by increasing the number of antennas, the performance is growing and the target tracking error is decreasing. In addition, by comparing Case3 and Case4 (symmetric geometry) with Case5 (asymmetric geometry), it is obvious that the symmetric configuration has better performance. (Note that in the all figures and scenarios, the unit of CRB and MSE is m^2).

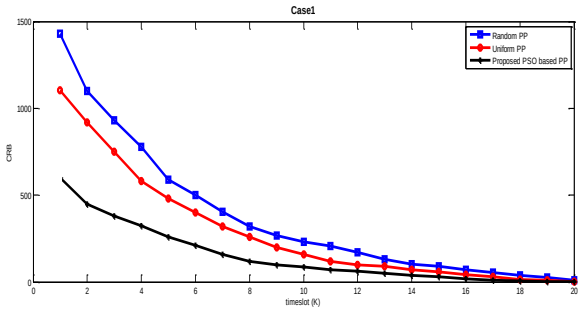

(a)

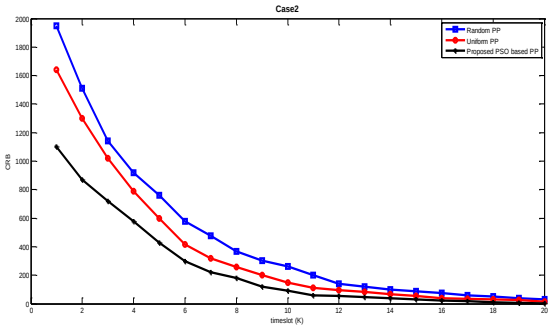

(b)

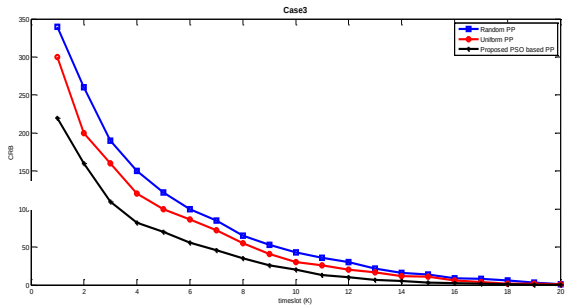

(c)

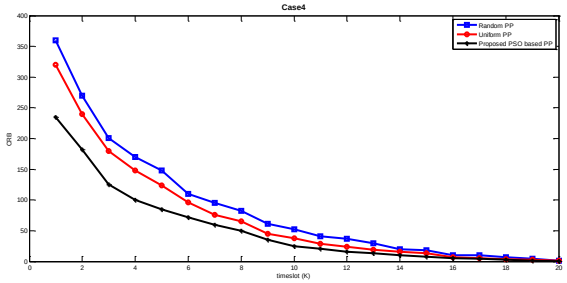

(d)

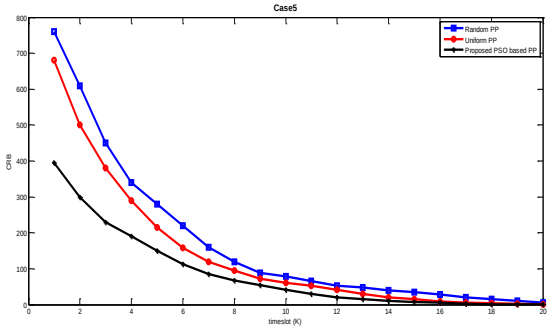

(e)

Fig.7. The Proposed Power Allocation Scheme (based on PSO) Comparison with Random and Uniform Power Allocation Schemes in the all Five Cases

To verify the accuracy of the proposed target tracking schemes, Fig.8 illustrates the tracking MSE and joint CRB in five Cases. The MSE is calculated as:

$$\mathrm{MSE_k} = \frac{1}{N_{MC}} \sum_{i=1}^{N_{MC}} trace(\boldsymbol{\Upsilon}_k(\boldsymbol{\theta}_k - \widehat{\boldsymbol{\theta}}_k^j)(\boldsymbol{\theta}_k - \widehat{\boldsymbol{\theta}}_k^j)^T \boldsymbol{\Upsilon}_k^T) \quad (67)$$

Where N_{MC} is the Monte Carlo number and $\widehat{\boldsymbol{\theta}}_k^j$ is the state estimate in the jth cycle. The joint CRB and MSE results in Fig.8, shows that the proposed tracking scheme results is close to actual conditions. This is true in the all five cases.

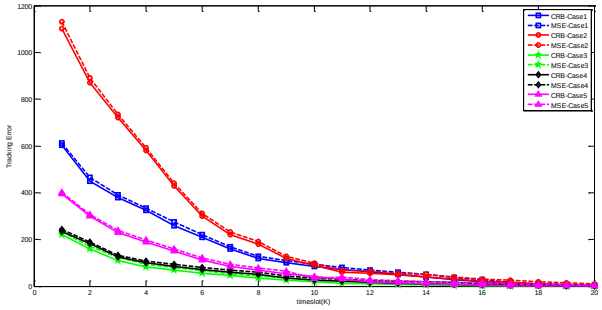

Fig.8. Tracking Errors in Five Cases with Proposed Target Tracking procedure (based on PSO)

In addition, Fig.8 shows that Case3 has the least tracking error and it is the best case. And also, the asymmetric Case5 has the better performance than Case1 and Case2 because the number of antennas in this case is more than those two cases. But in equal number of antennas, the symmetric Cases (Case3 and Case4) has the less target tracking error than asymmetric Case5. In Fig.9. we compare the joint CRB of the tracking error of the proposed power allocation scheme (based on PSO) is compared with the Exhaustive search method [16], which is the best algorithm for finding the result because it considers all possible conditions. This comparison is performed the best Case, Case3.

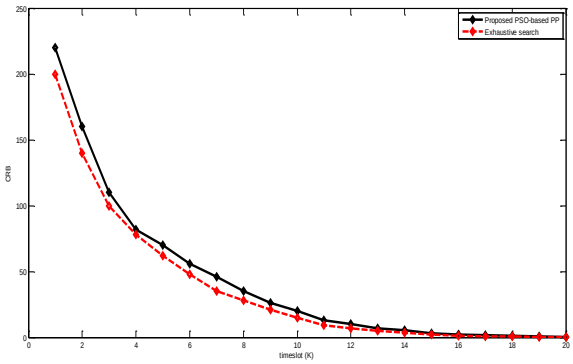

Fig.9. The Proposed Power Allocation scheme in Target Tracking (based on PSO) and Exhaustive Search Performance Comparison in Case3

By attention to Fig.9, it is clear that the proposed scheme result (based on PSO) for Case3 is near to the Exhaustive search method. This can prove the accuracy of the proposed strategy. However, the Exhaustive search has a high computational complexity and it takes about 49583 seconds. However, the proposed scheme (based on PSO) takes 804 seconds. The simulations are run in the system with Intel(R) core(TM) i7-3612QM CPU @2.1GHz and 6 GB RAM. In addition, the number of possible variable P_m for exhaustive search equals 5. To verify the proposed scheme (based on PSO) results, we repeat the experiments with SQP algorithm. We use this algorithm for the best Case in the previous experiment, Case3. Fig.10 shows the joint CRB of tracking error in the proposed power allocation scheme (based on SQP) with uniform and

random power allocation strategies and also the proposed scheme based on PSO algorithm. This figure illustrates that the proposed scheme based on SQP has the best performance. But its results are very close to the proposed schemes based on PSO. This proves that our proposed scheme has high accuracy and performance.

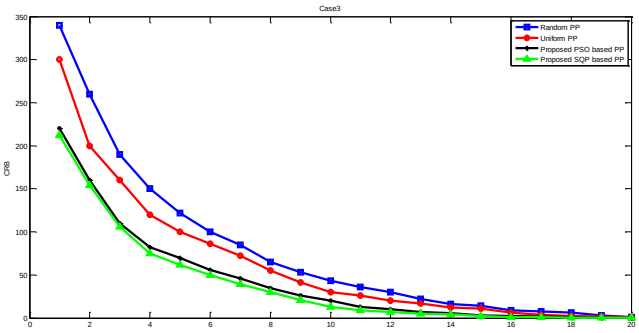

Fig.10. The Comparison of the Proposed power Allocation Scheme in Target Tracking (based on SQP) with Other Strategies in Case3

It should be emphasized that although the two SQP and PSO algorithm has the near performance for our proposed power allocation scheme in target tracking problem, but SQP has the less computational complexity than PSO and it takes 56.8612 seconds. Therefore, it is applicable in real-time scenarios. In Fig.11, the joint CRB of target tracking error of the proposed scheme (based on SQP) is compared with MSE. This shows that two results are near to each other. Therefore, the SQP based scheme is also close to real condition.

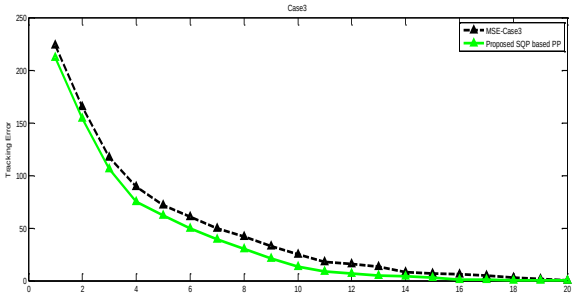

Fig.11 Target Tracking Error Evaluation in Case3 with Proposed Target Tracking Procedure (based on SQP algorithm)

6- Conclusions

The researchers should emphasize more in power allocation strategy on MIMO radar with widely dispersed antennas. Based on the limitations in the total power in the MIMO radar, the power allocation is critical.

In this manuscript, the power allocation scheme performance in widely separated MIMO radar is investigated. A complex Gaussian random RCS with different variance in each transmit-receive path is supposed. And also it is considered an unknown parameter. These are not considered in other papers and this condition is near to real. The simulation results prove that these assumptions enhance the radar performance.

Applying joint estimation of target velocity and position tracking error and also adding RCS estimation to the estimation state vector helps to improve the performance of this kind of MIMO radar. In simulations, five different Cases with symmetric and asymmetric antenna placement are considered to evaluate the proposed power allocation scheme for the target tracking problem in considered MIMO radar. This paper aims to form the power allocation scheme to minimize the tracking errors subject to the total transmit power and transmit power of each transmit antenna limitation. We proved that this problem is convex and used PSO and SQP algorithms to solve it. The simulation experiments are performed in various scenarios and the simulation proves the accuracy of the proposed scheme.

References

[1] M.A. Darzikolaei, A.Ebrahimzade, and E.Gholami, "Classification of radar clutters with artificial neural network." In 2015 2nd International Conference on Knowledge-Based Engineering and Innovation (KBEI), 2015, pp. 577-581.

[2] M.A. Darzikolaei, A.Ebrahimzade, and E.Gholami,"The Separation of Radar Clutters using Multi-Layer Perceptron.", Information Systems & Telecommunication, Vol.1, No.17,2017,pp 1-10.

[3] E. Fishler, A.Haimovich, R.Blum, D.Chizhik, L.Cimini, and R.Valenzuela,"MIMO radar: An idea whose time has come", In Proceedings of the 2004 IEEE Radar Conference (IEEE Cat. No. 04CH37509), , 2004, pp. 71-78.

[4] A. Pakdaman, and H.Bakhshi, "Separable transmit beampattern design for MIMO radars with planar colocated antennas", AEU-International Journal of Electronics and Communications, Vol.89, No.1, 2018,pp.153-159.

[5] M.J.Jahromi,and H.K.Bizaki, "Target Tracking in MIMO Radar Systems Using Velocity Vector",Journal of Information Systems and Telecommunication (JIST),Vol.3,No.7, 2014,pp. 150-158.

[6] S.H. Mostafavi-Amjad, V. Solouk, and H. Kalbkhani, "Energy-efficient user pairing and power allocation for granted uplink-NOMA in UAV communication systems", Journal of Information Systems and Telecommunication (JIST), Vol. 10, No. 40, 2014, pp.312-323.

[7] M. G. Adian, and H. Aghaeenia, "Joint relay selection and power allocation in MIMO cooperative cognitive radio networks", Journal of Information Systems and Telecommunication (JIST), Vol. 1, No. 9, 2015, pp.1-10.

[8] X.Mingchi, W.Yi, T.Kirubarajan, and L. Kong, "Joint node selection and power allocation strategy for multitarget tracking in decentralized radar networks", IEEE Transactions on Signal Processing, Vol.66, No. 3, 2017, pp.729-743.

[9] H. Godrich, A.P. Petropulu, and H. V.Poor,"Power allocation strategies for target localization in distributed multiple-radar architectures", IEEE Transactions on Signal Processing, Vol.59, No. 7, 2011,pp. 3226-3240.

[10] H.Chen, T.Shiying, and S.Bin,"Cooperative game approach to power allocation for target tracking in distributed MIMO radar sensor networks", IEEE Sensors Journal,Vol.15, No. 10, 2015, pp.5423-5432.
[11] M. Botao, H.Chen, S.Bin, and H,Xiao,"A joint scheme of antenna selection and power allocation for localization in MIMO radar sensor networks", IEEE communications letters, Vol.18, No. 12, 2014,pp.2225-2228.
[12] L.Yanxi, Z.He, X.Zhang, and S.Liu, "Transmit and receive sensors joint selection for MIMO radar tracking based on PCRLB", In 2016 IEEE 13th International Conference on Signal Processing (ICSP),2016, pp. 1551-1555.
[13] S.Xiyu, N.Zheng, and T.Bai,"Resource allocation schemes for multiple targets tracking in distributed MIMO radar systems",International Journal of Antennas and Propagation, Vol.2017 ,No.1,2017, pp.1-12.
[14] Y.Wei, Y.Yuan, R.Hoseinnezhad, and L.Kong,"Resource scheduling for distributed multi-target tracking in netted colocated MIMO radar systems", IEEE Transactions on Signal Processing, Vol.68, No.1, 2020, pp.1602-1617.
[15] Q. Cheng, J.Xie, and H.Zhang, "Joint Antenna Placement and Power Allocation for Target Detection in a Distributed MIMO Radar Network", Remote Sensing, Vol.14, No. 11,2022, pp.2650-2662.
[16] M.A. Darzikolaei, M.R. K.Mollaei, and M.Najimi,"An effective PSO-based power allocation for target tracking in MIMO radar with widely separated antennas", Physical Communication, Vol.51, No.1, 2022,pp.101544-101557.
[17] Y.Wei, Y.Yuan, R.Hoseinnezhad, and L.Kong. "Resource scheduling for distributed multi-target tracking in netted colocated MIMO radar systems",IEEE Transactions on Signal Processing, Vol.68, No.1, 2020,pp.1602-1617.
[18] L.Zhengjie, J.Xie, H.Zhang, H.Xiang, and Z.Zhang, "Adaptive sensor scheduling and resource allocation in netted collocated MIMO radar system for multi-target tracking", IEEE Access, Vol.8 ,No.1, 2020, pp.109976-109988.
[19] H. Qian, R.S. Blum, and A.M. Haimovich,"Noncoherent MIMO radar for location and velocity estimation: More antennas means better performance",IEEE Transactions on Signal Processing, Vol.58, No. 7, 2010,pp.3661-3680.
[20] E. Fishler, A.Haimovich, R.Blum, D.Chizhik, L.Cimini, and R.Valenzuela,"MIMO radar: An idea whose time has come", In Proceedings of the 2004 IEEE Radar Conference (IEEE Cat. No. 04CH37509), , 2004, pp. 71-78.
[21] C., and A.Nehorai,"Scheduling and power allocation in a cognitive radar network for multiple-target tracking",IEEE Transactions on Signal Processing,Vol.60, No. 2, 2012, pp.715-729.
[22] H.Godrich, A.M. Haimovich, and R.S. Blum,"Target localization accuracy gain in MIMO radar-based systems",IEEE Transactions on Information Theory, Vol.56, No. 6,2010, pp. 2783-2803.
[23] V.Trees, and L.Harry, Detection, estimation, and modulation theory, part I: detection, estimation, and linear modulation theory. John Wiley & Sons, 2004.
[24] S.Palin, J.Tang, Q.He, B.Tang, and X.Tang,"Cramer–Rao bound of parameters estimation and coherence performance for next generation radar",IET Radar, Sonar & Navigation, Vol.7, No. 5, 2013, pp.553-567.
[25] E.Russell, and J.Kennedy, "A new optimizer using particle swarm theory",In MHS'95. Proceedings of the Sixth International Symposium on Micro Machine and Human Science, 1995, pp. 39-43.
[26] S.Chenguang, Y.Wang, F.Wang, S.Salous, and J.Zhou,"Joint optimization scheme for subcarrier selection and power allocation in multicarrier dual-function radar-communication system", IEEE Systems Journal, Vol.15, No. 1 ,2020, pp. 947-958.
[27] S.Boyd, and L.Vandenberghe, Convex optimization, Cambridge university press, 2004.
[28] J.Yan, H.Liu, B.Jiu, and Z.Bao,"Power allocation algorithm for target tracking in unmodulated continuous wave radar network", IEEE sensors journal, Vol.15, No. 2 , 2014,pp.1098-1108.

Appendix I.

If we do not consider noise, we will have $r_{mn,k}(t) = \sqrt{P_m}\ \xi_{mn,k}\ s_m\big(t-\tau_{mn,k}\big)\ e^{j2\pi f_{mn,k}t}$, therefore for two independent paths:

$$\mathrm{L}_J\big(\boldsymbol{\theta}_k;\boldsymbol{r}(t)\big) = \sum_{m=1}^{M}\sum_{n=1}^{N}\Big(-\ln\big(\sigma_{mn,k}^2P_m+1\big) + \frac{\sigma_{mn,k}^4P_m^2}{\sigma_{mn,k}^2P_m+1}\Big|\int_{-\infty}^{+\infty} s_m\big(t-\tau_{m'n',k}\big)\ s_m^*\big(t-\tau_{mn,k}\big)e^{+j2\pi(f_{m'n',k}-f_{mn,k})t}\,dt\Big|^2\Big) \tag{A.1}$$

And

$$\mathrm{G}_{13=} -\frac{\partial}{\partial\sigma_{mn,k}^2}\cdot\frac{\partial}{\partial\tau_{mn,k}}\mathrm{L}_J\big(\boldsymbol{\theta}_k;\boldsymbol{r}(t)\big) = -\frac{\partial}{\partial\sigma_{mn,k}^2}\frac{\sigma_{mn,k}^4P_m^2}{\sigma_{mn,k}^2P_m+1}\cdot\frac{\partial}{\partial\tau_{mn,k}}\sum_{m=1}^{M}\sum_{n=1}^{N}\Big|\int_{-\infty}^{+\infty} s_m\big(t-\tau_{m'n',k}\big)\ s_m^*\big(t-\tau_{mn,k}\big)e^{+j2\pi\left(f_{m'n',k}-f_{mn,k}\right)t}\,dt\Big|^2\Big) \tag{A.2}$$

And also by considering

$$\frac{\partial}{\partial\sigma_{mn,k}^2}\frac{\sigma_{mn,k}^4P_m^2}{\sigma_{mn,k}^2P_m+1} \approx \frac{\sigma_{mn,k}^2P_m^2}{\sigma_{mn,k}^2P_m+1} \tag{A.3}$$

And

$$\frac{\partial}{\partial\tau_{mn,k}}\sum_{m=1}^{M}\sum_{n=1}^{N}\Big|\int_{-\infty}^{+\infty} s_m\big(t-\tau_{m'n',k}\big)\ s_m^*\big(t-\tau_{mn,k}\big)e^{+j2\pi\left(f_{m'n',k}-f_{mn,k}\right)t}\,dt\Big|^2\Big) =$$

$$-2\Big(\int_{-\infty}^{+\infty} s_m\big(t-\tau_{m'n',k}\big)\frac{\partial s_m^*\big(t-\tau_{mn,k}\big)}{\partial\tau_{mn,k}}\ e^{+j2\pi\left(f_{m'n',k}-f_{mn,k}\right)t}\,dt\Big)\cdot\Big(\int_{-\infty}^{+\infty} s_m\big(t-\tau_{m'n',k}\big)\ s_m^*\big(t-\tau_{mn,k}\big)e^{+j2\pi\left(f_{m'n',k}-f_{mn,k}\right)t}\,dt \tag{A.4}$$

Based on the paper assumptions and **Appendix II** and by considering $(m=m', n=n')$:

$$\int_{-\infty}^{+\infty} s_m(t - \tau_{m'n',k}) \frac{\partial s_m^*(t-\tau_{mn,k})}{\partial \tau_{mn,k}} e^{+j2\pi\left(f_{m'n',k}-f_{mn,k}\right)t}\, dt = \int_{-\infty}^{+\infty} s_m(t-\tau_{mn,k}) \frac{\partial s_m^*(t-\tau_{mn,k})}{\partial \tau_{mn,k}}\, dt \xrightarrow{D.2} -j2\pi \int f|S_m(f)|^2 df \quad (A.5)$$

And also,

$$\int_{-\infty}^{+\infty} s_m\left(t-\tau_{m'n',k}\right)\ s_m^*\left(t - \tau_{mn,k}\right)e^{+j2\pi\left(f_{m'n',k}-f_{mn,k}\right)t}\, dt = \int_{-\infty}^{+\infty} s_m\left(t-\tau_{mn,k}\right)\ s_m^*\left(t-\tau_{mn,k}\right) dt \xrightarrow{D.1} 1 \quad (A.6)$$

Therefore:

$$G_{13} = G_{31} = -\frac{\sigma_{mn,k}^2 P_m^2}{\sigma_{mn,k}^2 P_m + 1}.(-2).-j2\pi \int f|S_m(f)|^2 df = -j4\pi \frac{\sigma_{mn,k}^2 P_m^2}{\sigma_{mn,k}^2 P_m + 1}\left(\int f|S_m(f)|^2 df\right) \quad (A.7)$$

And also, G_{23}, G_{32} ,and G_{33} are obtained in the same method as:

$$G_{23} = G_{32} = j4\pi\left(\frac{\sigma_{mn,k}^2 P_m^2}{\sigma_{mn,k}^2 P_m + 1}\right).\left(\int_{-\infty}^{+\infty} t \mid s_m^*(t - \tau_{mn,k})\right|^2 dt\Bigg) \quad (A.8)$$

$$\mathrm{G}_{33} == \frac{2P_m^2}{\left(\sigma_{mn,k}^2 P_m + 1\right)^2} \quad (A.9)$$

Since we want to compute FIM and we can choose greater value, and for simplicity we choose $\frac{2P_m^2}{\sigma_{mn,k}^2 P_m+1}$ for G_{33}.

Appendix II.

If the signals are orthogonal [24], they may have the below conditions:

$$\int_T s_k(t)\ s_m^*(t)\, dt \approx \begin{cases} 1 & k = m \\ 0 & k \neq m \end{cases} \quad (B.1)$$

$$\int_T s_k(t-\tau_{lk})\ \dot{s}_k^*(t-\tau_{lk})\, dt = -j2\pi \int f|S_k(f)|^2 df \quad (B.2)$$

$$\int_T |\dot{s_k}(t)|^2\, dt = 4\pi^2 \int f^2|S_k(f)|^2 df \quad (B.3)$$

Appendix III.

we should check the convexity of (46). First, we simplify the problem:

$$\mathbf{J}_{\mathrm{D}}(\boldsymbol{\theta}_{\mathrm{k}}) = \sum_{m=1}^{M-}\sum_{n=1}^{N} 8\pi^2\left(\sigma_{mn}^2 P_m - 1\right).(\mathrm{G_{mn}})_{5\times5} + \sum_{m=1}^{M}\sum_{n=1}^{N} 8\pi^2\ \frac{+1}{\sigma_{mn}^2 P_m + 1}.(\mathrm{G_{mn}})_{5\times5} \quad (C.1)$$

The objective function is as $trace(\mathbf{J}_{\mathrm{D}}^{-1}(\boldsymbol{\theta}_{\mathrm{k}}))$. For proof the convexity, if we suppose objective function as$G(P_m)$, by choosing two value P_m and $P_{m'}$ then we should be have $G(\alpha P_m + (1-\alpha)P_{m'}) \leq \alpha G(P_m) + (1-\alpha)G(P_{m'})$[25].

$$G(P_m) \approx trace\left(\left\{\sum_{m=1}^{M}\sum_{n=1}^{N} 8\pi^2\left(\sigma_{mn}^2 P_m - 1\right).(\mathrm{G_{mn}})_{5\times5} + \sum_{m=1}^{M}\sum_{n=1}^{N} 8\pi^2\ \frac{+1}{\sigma_{mn}^2 P_m + 1}.(\mathrm{G_{mn}})_{5\times5}\right\}^{-1}\right) \quad (C.2)$$

Since the objective function is as $trace(\boldsymbol{X}^{-1})$, for proof convexity, the $\boldsymbol{X}$ should be affine [28]. First, we investigate the convexity of $\sum_{m=1}^{M}\sum_{n=1}^{N} 8\pi^2\left(\sigma_{mn}^2 P_m - 1\right).(\mathrm{G_{mn}})_{5\times5}$:

$$G_1'(P_m) = \sum_{m=1}^{M}\sum_{n=1}^{N} 8\pi^2\left(\sigma_{mn}^2 P_m - 1\right).(\mathrm{G_{mn}})_{5\times5}$$

$$\rightarrow G_1'(\alpha P_m + (1-\alpha)P_{m'}) = \sum_{m=1}^{M}\sum_{n=1}^{N} 8\pi^2\left(\sigma_{mn}^2(\alpha P_m + (1-\alpha)P_{m'}) - 1\right).(\mathrm{G_{mn}})_{5\times5}$$

$$= \alpha \sum_{m=1}^{M}\sum_{n=1}^{N} 8\pi^2\left(\left(\sigma_{mn}^2(P_m) - 1\right)\right).(\mathrm{G_{mn}})_{5\times5} + (1-\alpha)\sum_{m=1}^{M}\sum_{n=1}^{N} 8\pi^2\left(\left(\sigma_{mn}^2(P_{m'}) - 1\right)\right).(\mathrm{G_{mn}})_{5\times5}$$

$$= \alpha G_1'(\alpha P_m) + (1-\alpha)G_1'(P_{m'})) \quad (C.3)$$

Therefore, $G_1'(P_m)$ is convex.For the next part:

$$G_2(P_m) = \sum_{m=1}^{M}\sum_{n=1}^{N} 8\pi^2\ \frac{+1}{\sigma_{mn}^2 P_m + 1}.(\mathrm{G_{mn}})_{5\times5} \quad (C.4)$$

Therefore,

$$G_2(\alpha P_m + (1-\alpha)P_{m'}) = \sum_{m=1}^{M}\sum_{n=1}^{N} 8\pi^2\left(\sigma_{mn}^2(\alpha P_m + (1-\alpha)P_{m'}) + 1\right)^{-1}.(\mathrm{G_{mn}})_{5\times5} = \sum_{m=1}^{M}\sum_{n=1}^{N} 8\pi^2\left(\sigma_{mn}^2\alpha(P_m + 1) + \sigma_{mn}^2(1-\alpha)(P_{m'} + 1)\right)^{-1}.(\mathrm{G_{mn}})_{5\times5} \quad (C.5)$$

Therefore, with respect to the value of P_m and parameters of our problem, the condition $(A+B)^{-1} \leq A^{-1} + B^{-1}$ is satisfied for (C.5) and we will have:

$$\sum_{m=1}^{M}\sum_{n=1}^{N} 8\pi^2\,(\sigma_{mn}^2\alpha(P_m+1)+\sigma_{mn}^2(1-\alpha)(P_{m'}+1))^{-1}.(\mathrm{G_{mn}})_{5\times5} \le \alpha * \sum_{m=1}^{M}\sum_{n=1}^{N} 8\pi^2\,(\sigma_{mn}^2(P_m+1)^{-1}.(\mathrm{G_{mn}})_{5\times5} + (1-\alpha) * \sum_{m=1}^{M}\sum_{n=1}^{N} 8\pi^2\,(\sigma_{mn}^2(P_{m'}+1)^{-1}.(\mathrm{G_{mn}})_{5\times5} = \alpha * G_2(P_m) + (1-\alpha) * G_2(P_{m'}) \quad \text{(C.6)}$$

Therefore $G_2(P_m)$ is also convex. Then we can conclude that $G(P_m)$ is convex and in result, our problem is convex.